Design of Biorthogonal Wavelets based on Spline and Spline-like Functions for Image Compression

[1]K Subramanyam, [2]T Ramasri
[1]Assistant Professor, Dept. of ECE, Gokula Krishna College of Engineering, Sullurpet
[2]Professor, Dept. of ECE, Sri Venkateswara University College of Engineering, Tirpati

Abstract—Wavelet theory inspired from Fourier analysis is based on the basis function and its properties. Different wavelets use different basis functions which may better suit to some applications. The properties of basis functions along with their shape and magnification effects the performance of an application. The standard biorthogonal wavelets utilize spline functions for their construction. In this paper first the design procedure of biorthogonal wavelets is presented. Then a modified spline function is proposed. Based on the proposed spline function, three biorthogonal wavelets are designed with different length. The performance of proposed wavelets is analyzed by applying them on to images for SPIHT compression. The simulation results shown that the proposed wavelets have performed well compared to that of standard spline based biorthogonal wavelets.

Index Terms— spline-like function, biorthogonality, symmetry, normality.

1 Introduction

Though wavelets are treated as basic domain transformation technique, these have many features that a traditional transformation scheme doesn't have. The first thing to note is that the basis function is unique [1]. For that matter, when compared with regular transformation schemes like Fourier Transformation, the wavelet transform itself is unique. Haar wavelet is different from Daubechies wavelet and symlet is different from coiflet. The reason is the basis function different [2]-[5]. It is noteworthy that the transformation style is same for all the wavelets. When a comparison is made with Fourier transformation, Fourier transformation is only one transform, one structure and one basis function.

The operations like translation and dilation will be performed on the scaling and wavelet functions and the resulting waveforms will be used to find out the similarity with the input signal at hand. The similarity measure termed as wavelet domain will be utilized in inverse wavelet transform to get the original signal back without any deviation. Hence, the similarity measure plays major role in whole success of the wavelet transforms. Many researchers changed the basis function of the wavelet transform as per their view and requirement, resulting in varied wavelets and wavelet transforms [6][7].

Apart from basis function, wavelets are different among themselves based whether same set of waveforms are being used in decomposition and reconstruction or not. Orthogonal wavelets use same set of scaling and wavelet functions at both decomposition and reconstruction end. On the other hand, biorthogonal wavelet uses different set of scaling and wavelet function at forward and inverse ends of the transformation. With biorthogonal wavelets, the design flexibility has increased tremendously to design as many wavelets as one desire as well as many wavelets as a specific application need. In the standard biorthogonal wavelets, spline functions are used to devise scaling and wavelet functions. Based on length of these function, further classes of wavelets are being designed. In this paper, the design process of wavelets with the help of spline-like functions is proposed and simulation results of image compression using proposed wavelets is presented [8]-[11].

2 Design of Biorthogonal Wavelets based on Spline-like Functions

The standard Spline function is defined as follows.

$$N_k(t) = \sum_{i=0}^{k} p_i N_k(2t-i)$$

where $$p_i = \frac{1}{2^{k-1}} \binom{k}{i}.$$

Here the p_i is the scaling value of dilated and translated spline function. The scaling value is directly proportional to binomial coefficients. Hence symmetry is guaranteed [12]. The coefficients are linearly distributed. Now a modified Spline is proposed. The new spline-like function is supposed to have symmetry but the coefficient values are modified to have more weight at center and gradually approaches standard spline function. The p_i is modified and given below [13]-[15].

For $i \le (k/2)$, $p_i = \frac{i+1}{2^{k-1}} \binom{k}{i}$ and

for $i > (k/2)$, $p_i = \frac{k-i+1}{2^{k-1}} \binom{k}{i}$.

The coefficients of the standard Spline and proposed Spline-like functions are given in Fig. 1.

 https://doi.org/10.58482/ijeresm.v1i1.3

Standard Spline	Proposed Spline-like
1	1
1 1	1 1
1 2 1	1 4 1
1 3 3 1	1 6 6 1
1 4 6 4 1	1 8 18 8 1
1 5 10 10 5 1	1 10 30 30 10 1

Fig. 1 Coefficients of standard Spline function and proposed Spline-like function

In Fig. 1, the coefficients are given by ignoring the division by 2^{k-1}. By using the above spline-like function with different lengths three wavelets are designed. These are denoted by 'biorsl12', 'biorsl23' and 'biorsl34' respectively.

The spline-like functions of length 3, 5 and 7 are utilized for 'biorsl12', 'biorsl23' and 'biorsl34' respectively. The normalized coefficients of the spline-like function used for the wavelet 'biorsl12' (k=2) are given below.

$$h(-1)=p_0=\frac{\sqrt{2}}{6},\quad h(0)=p_1=\frac{2\sqrt{2}}{3},\quad h(1)=p_2=\frac{\sqrt{2}}{6}$$

Similarly the coefficients for 'biorsl23' (k=4) and 'biorsl34' (k=6) are given below.

$$h(-2)=p_0=\frac{2\sqrt{2}}{72},\quad h(-1)=p_1=\frac{2\sqrt{2}}{9},\quad h(0)=p_2=\frac{\sqrt{2}}{2},\quad h(1)=p_3=\frac{2\sqrt{2}}{9},\quad h(2)=p_4=\frac{2\sqrt{2}}{72}.$$

$$h(-3)=p_0=\frac{\sqrt{2}}{196}, h(-2)=p_1=\frac{3\sqrt{2}}{49}, h(-1)=p_2=\frac{45\sqrt{2}}{196}, h(0)=p_3=\frac{20\sqrt{2}}{49},$$

$$h(1)==p_4\frac{45\sqrt{2}}{196}, h(2)=p_5=\frac{3\sqrt{2}}{49}, h(-3)=p_6=\frac{\sqrt{2}}{196}$$

Using the property of double shift biorthogonality, normality, symmetry and vanishing moments the following equations are derived for 'biorsl12'.

$$2\tilde{h}(-2)+2\tilde{h}(-1)+\tilde{h}(0)=\sqrt{2}$$

$$2\tilde{h}(-2)-2\tilde{h}(-1)+\tilde{h}(0)=0$$

$$\tilde{h}(-1)+2\tilde{h}(0)=3/\sqrt{2}$$

$$\tilde{h}(-1)+4\tilde{h}(-2)=0$$

The unique solution to the above system of equations is given below.

$$\tilde{h}(-2)=-\frac{\sqrt{2}}{16},\quad \tilde{h}(-1)=\frac{\sqrt{2}}{4},\quad \tilde{h}(0)=\frac{5\sqrt{2}}{8},\quad \tilde{h}(1)=\frac{\sqrt{2}}{4},\quad \tilde{h}(2)=-\frac{\sqrt{2}}{16}.$$

Similarly the coefficients for 'biorsl23' and 'biorsl34' are calculated and the coefficients of 'coifsl34' are given below.

$$\tilde{h}(-3)=-\frac{5\sqrt{2}}{256}, \tilde{h}(-2)=-\frac{5\sqrt{2}}{32}, \tilde{h}(-1)=\frac{59\sqrt{2}}{256}, \tilde{h}(0)=\frac{13\sqrt{2}}{16},$$

$$\tilde{h}(1)=\frac{59\sqrt{2}}{256}, \tilde{h}(2)=-\frac{5\sqrt{2}}{32}, \tilde{h}(3)=-\frac{5\sqrt{2}}{256}$$

The coefficients of 'coifsl34' are given below.

$$\tilde{h}(-4)=-\frac{\sqrt{2}}{128}, \tilde{h}(-3)=\frac{3\sqrt{2}}{32}, \tilde{h}(-2)=-\frac{5\sqrt{2}}{16}, \tilde{h}(-1)=\frac{5\sqrt{2}}{32}, \tilde{h}(0)=\frac{73\sqrt{2}}{64},$$

$$\tilde{h}(1)=\frac{5\sqrt{2}}{32}, \tilde{h}(2)=-\frac{5\sqrt{2}}{16}, \tilde{h}(3)=\frac{3\sqrt{2}}{32}, \tilde{h}(4)=-\frac{\sqrt{2}}{128}.$$

The above are scaling function coefficients at decomposition and reconstruction side. The wavelet function coefficients are calculated from these values using expressions presented in previous sections. The wavelet and scaling functions of the proposed wavelets are plotted in the Fig. 2, 3 and 4.

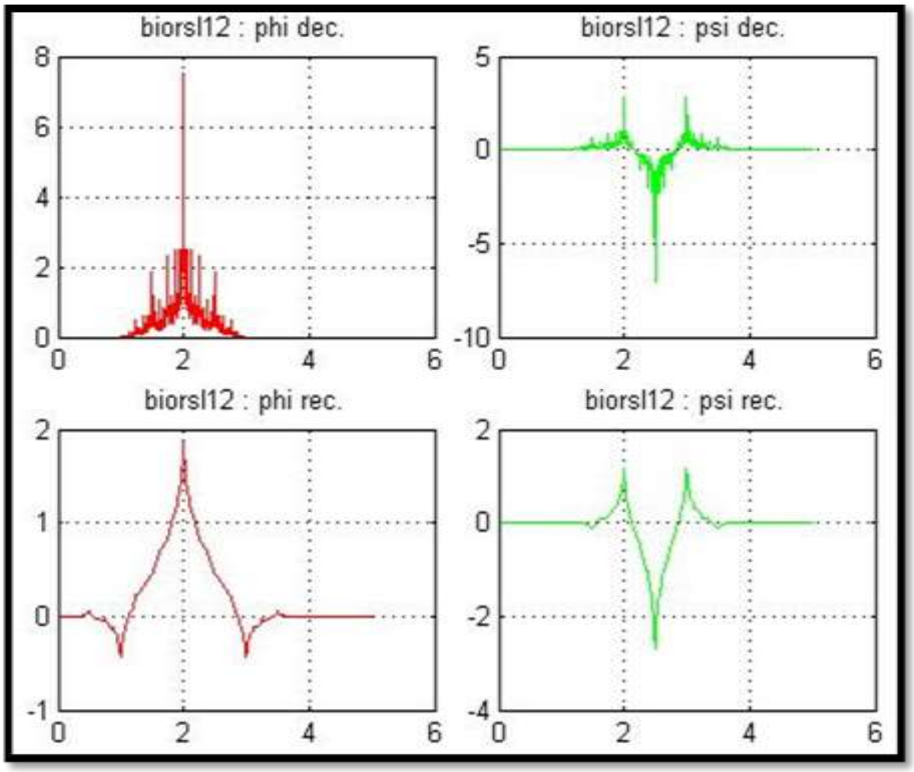

Fig. 2 Wavelet and scaling functions associated with 'biorsl12'

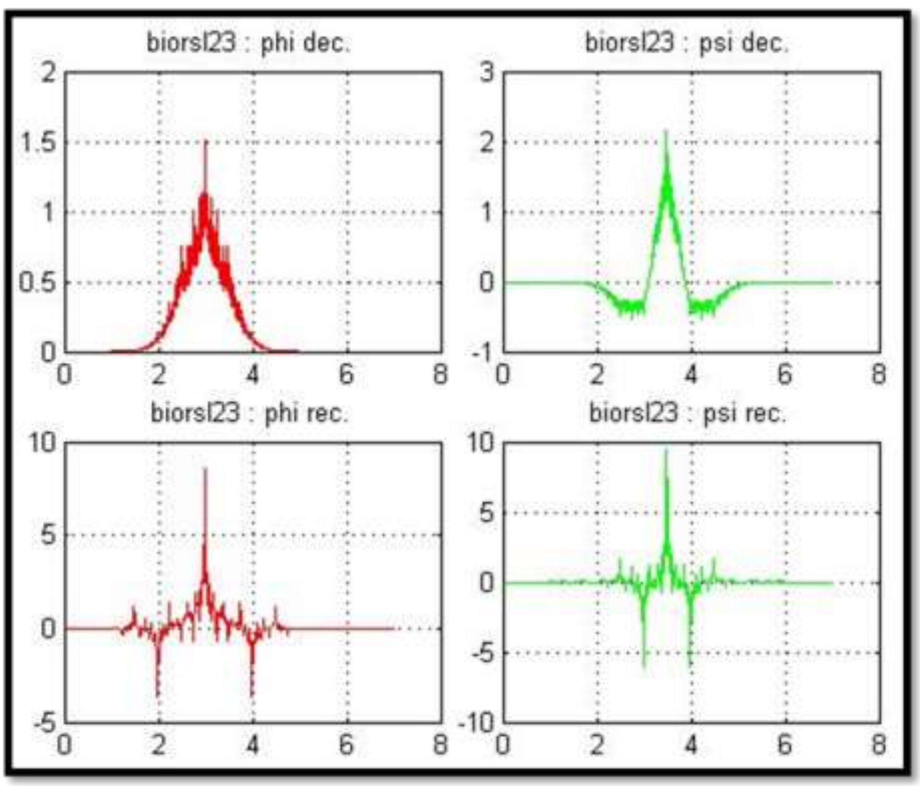

Fig. 3 Wavelet and scaling functions associated with 'biorsl23'

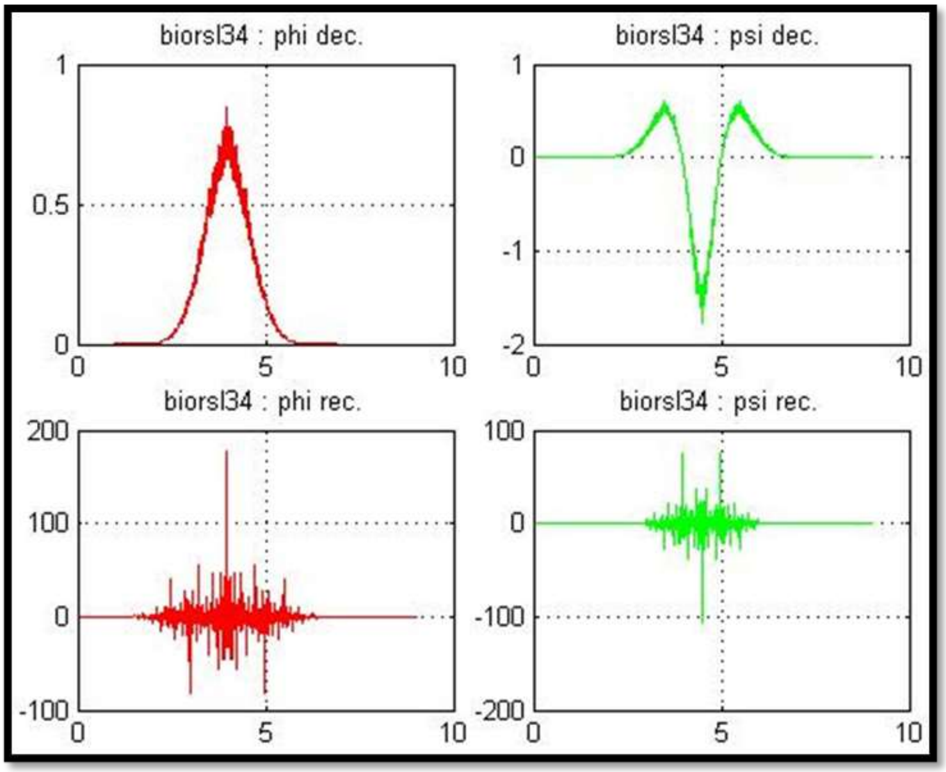

Fig. 4 Wavelet and scaling functions associated with 'biorsl34'

3 Simulation Results

In this work a total of six wavelets are designed. Out of these six wavelets, three wavelets are based on the standard spline functions. The remaining three wavelets are based on modified spline or spline-like function described in the previous section. The first three wavelets are denoted by 'biors12', 'biors23' and 'biors34'. The spline-like function-based wavelets are denoted by 'biorsl12', 'biorsl23' and 'biorsl34'. In this section, the designed wavelets are used for image compression. SPIHT coding was utilized for compression of images. Tables 1 and 2 shows the compression ratio and PSNR values using different wavelets.

Table 1 CR Values obtained using different wavelets

COMPRESSION RATIO										
Wavelet/Image	BMI	cameraman	ct	greens	lena	MI	NI	pepper	rice	SI
Spline12	2.22	2.33	3.32	1.94	2.48	2.44	2.13	2.57	2.60	1.86
Spline23	1.94	1.96	3.10	1.74	2.13	2.06	1.80	2.19	2.20	1.60
Spline34	1.47	1.56	2.41	1.36	1.66	1.66	1.45	1.58	1.74	1.32
Spline-like12	2.32	2.40	3.37	2.01	2.60	2.52	2.19	2.71	2.74	1.91
Spline-like23	2.14	2.25	3.27	1.88	2.38	2.36	2.06	2.46	2.47	1.80
Spline-like34	1.94	1.95	3.08	1.73	2.14	2.19	1.89	2.14	2.19	1.59

Table 2 PSNR Values obtained using different wavelets

PEAK SIGNAL TO NOISE RATIO										
Wavelet/Image	BMI	cameraman	ct	greens	lena	MI	NI	pepper	rice	SI
Spline12	25.8	27.5	33.5	24.6	33.4	27.6	26.7	32.2	35.5	21.8
Spline23	18.6	21.7	27.2	18.7	26.1	20.5	20.7	24.9	26.9	16.0
Spline34	16.9	18.1	24.3	10.3	17.5	12.6	16.7	17.7	18.0	10.0
Spline-like12	27.7	28.9	34.6	26.2	34.8	29.6	28.1	34.0	36.9	23.4
Spline-like23	26.4	28.9	34.7	26.1	33.1	28.5	28.0	32.4	34.2	23.3
Spline-like34	32.5	34.6	40.6	26.6	34.4	32.3	31.8	34.7	34.7	27.4

Fig. 2 and 3 plot the CR and PSNR values tabulated in tables 1 and 2. Based on the length of the functions it is correct to compare ‘biors12’ with ‘biorsl12’ etc. To analyze effectiveness of proposed spline-like functions. Any wavelet can be compared with any other wavelet to check the usefulness of a wavelet in compressing images. In the case of spline-based wavelets the compression measures both CR and PSNR are decreasing as the length of spline function increases. In the case of spline-like function-based wavelets the compression ratio decreases as the length spline-like function increases but PSNR varies differently. Simulation results of about 10 images are presented.

Out of these poor results are recorded for ‘greens’ image. CR of 1.94, 1.74, 1.36 and PSNR of 24.6dB, 18.7dB, 10.3dB are obtained using ‘biors12’, ‘biors23’ and ‘biors34’ respectively. CR of 2.01, 1.88, 1.73 and PSNR of 26.2dB, 26.1dB, 26.6dB are obtained using ‘biorsl12’, ‘biorsl23’ and ‘biorsl34’ respectively. Better results are recorded for ‘CT Scan’ image. CR of 3.32, 3.10, 2.41 and PSNR of 33.5dB, 27.2dB, 24.3dB are obtained using ‘biors12’, ‘biors23’ and ‘biors34’ respectively. CR of 3.37, 3.27, 3.08 and PSNR of 34.6dB, 34.7dB, 40.6dB are obtained using ‘biorsl12’, ‘biorsl23’ and ‘biorsl34’ respectively.

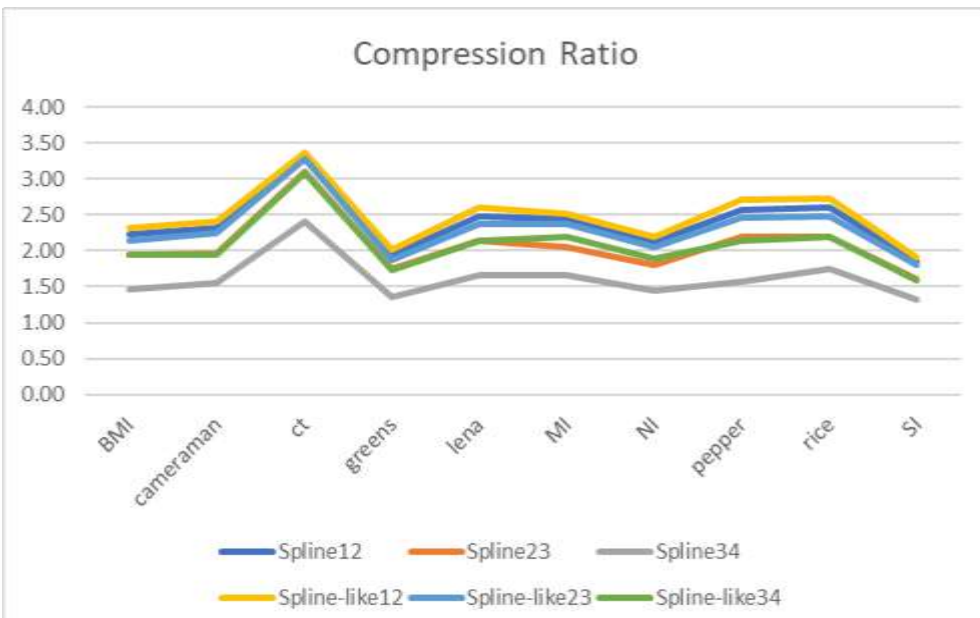

Fig. 2 CR Values obtained using different wavelets

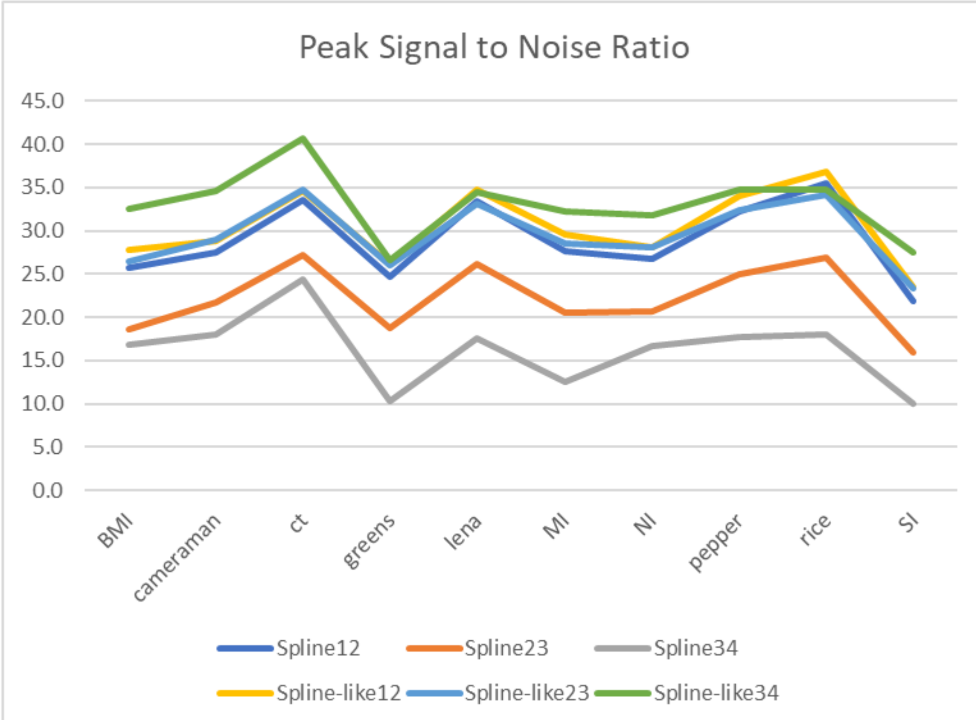

Fig. 3 PSNR Values obtained using different wavelets

4 Conclusions

Biorthogonal wavelets being more flexible for design are in use in wide variety of applications. The interesting feature of biorthogonal wavelet is that giving multiple degrees of freedom to realize the wavelet transform more over realizing the real meaning of the wavelet transform itself. In this paper in addition to the presentation of construction of biorthogonal wavelet transform, new basis functions are proposed and realized the biorthogonal wavelet transforms using the new basis functions. The new wavelet transforms are verified with the perfect reconstruction conditions practically by applying to images. Then these wavelets are used for compressing images using the algorithm of SPIHT. The simulation results presented proved the superiority of the proposed wavelets.

References

[1] N. Abmed and K. R. Rao, "Orthogonal Transforms for Digital Signal Processing", Springer Press, Berlin, (1975), pp. 1-10.

[2] B. Shen and I. K. Sethi, "DCT convolution and its application in compressed domain", IEEE Transactions on Circuits and Systems for Video Technology, vol. 8, no. 8, (1998), pp. 947-952.

[3] Z. X. Hou and X. Yang, "The all phase DFT filter", Proceedings of the 10th IEEE Digital Signal Processing Workshop and the 2nd IEEE Signal Processing Education Workshop, Pine Mountain, Georgia, USA, (2002), October 13-16, pp. 221-226.

[4] Z. X. Hou, Z. H. Wang and X. Yang, "Design and implementation of all phase DFT digital filter", Acta Electronica Sinica, vol. 31, no. 4, (2003), pp. 539-543.

[5] Z. X. Hou, "Design and application of the discrete cosine sequency filters", Journal of Tianjin University (Science and Technology), vol. 32, no. 3, (1999), pp. 324-328.

[6] S. G. Mallat, "A theory for multiresolution signal decomposition: The wavelet representation", IEEE Transactions on Pattern Analysis and Machine Intelligence, vol. 11, no. 7, (1989), pp. 674-693.

[7] S. G. Mallat, "Multiresolution approximations and wavelet orthonormal bases of *L*2(R)", Transactions of the American Mathematical Society, vol. 315, no. l, (1989), pp. 69-87.

[8] D. L. Donoho, "De-noising by soft-thresholding", IEEE Transactions on Information Theory, vol. 41, no. 3, (1995), pp. 613-627.

[9] D. Taubman, "High performance scalable image compression with EBCOT", IEEE Transactions on Image Processing, vol. 9, no. 7, (2000), pp. 1158-1170.

[10] Junqiu Wang, Juanfei Li, "Existence and Design of a Kind of Biorthogonal Vector-Valued Wavelets", IEEE International Conference on Environmental Science and Information Application Technology, vol. 3, 2009.

[11] Jian-Zhong Liu, Zheng-Xin Hou, Cheng-you Wang, "Design and properties of anti-symmetric biorthogonal wavelet filter banks with the same even length", IEEE International Conference on Wavelet Analysis and Pattern Recognition, 2009.

[12] Manish Sharma, Tarwar Sinrgh, Dinesh Bhati, Vikram Gadre, "Design of two-channel linear phase biorthogonal wavelet filter banks via convex optimization", IEEE International Conference on Signal Processing and Communications (SPCOM), 2014.

[13] HUANG Jing, LV Bing-qing, "A Feasible Algorithm for Designing Biorthogonal Bivariate Vector-valued Finitely Supported Wavelets", International Conference on Solid State Devices and Materials Science, ELSEVIER Physics Procedia, 25, 1507 – 1514, 2012.

[14] Delin Hua, Construction of a type of Biorthogonal Binary Wave Functions by Multiresolution Analysis Approach", International Conference on Solid State Devices and Materials Science, ELSEVIER Physics Procedia, 33, 1346 – 1353, 2012.

[15] Hongli Shi and Shuqian Luo, "A New Scheme for the Design of Hilbert Transform Pairs of Biorthogonal Wavelet Bases", EURASIP Journal on Advances in Signal Processing 2010.